The Journal of Infectious Diseases

MAJOR ARTICLE

Disease-specific differences in pharmacokinetics of paromomycin and miltefosine between post-kala-azar dermal leishmaniasis and visceral leishmaniasis patients in eastern Africa

Wan-Yu Chu[1,2], Luka Verrest[2], Brima M. Younis[3], Ahmed M. Musa[3], Jane Mbui[4], Rezika Mohammed[5], Joseph Olobo[6], Koert Ritmeijer[7], Séverine Monnerat[8], Monique Wasunna[9], Ignace C. Roseboom[2], Alexandra Solomos[8], Alwin D.R. Huitema[2,10,11], Fabiana Alves[8], Thomas P.C. Dorlo[1]

[1] Department of Pharmacy, Uppsala University, Uppsala, Sweden; [2] Department of Pharmacy and Pharmacology, Netherlands Cancer Institute, Amsterdam, the Netherlands; [3] Institute of Endemic Diseases, University of Khartoum, Khartoum, Sudan; [4] Kenya Medical Research Institute, Nairobi, Kenya; [5] Leishmaniasis Research and Treatment Center, University of Gondar, Gondar, Ethiopia; [6] Makerere University, Kampala, Uganda; [7] Médecins Sans Frontières, Amsterdam, the Netherlands; [8] Drugs for Neglected Diseases initiative, Geneva, Switzerland; [9] Drugs for Neglected Diseases initiative, Nairobi, Kenya; [10] Department of Pharmacology, Princess Máxima Center for Pediatric Oncology, Utrecht, the Netherlands; [11] Department of Clinical Pharmacy, University Medical Center Utrecht, Utrecht University, Utrecht, the Netherlands

Treatment regimens for post-kala-azar dermal leishmaniasis (PKDL) are usually extrapolated from those for visceral leishmaniasis (VL), but drug pharmacokinetics (PK) can differ due to disease-specific variations in absorption, distribution, and elimination. This study characterized PK differences in paromomycin and miltefosine between 109 PKDL and 264 VL patients from eastern

Corresponding author: Thomas P.C. Dorlo, Department of Pharmacy, *Pharmacometrics for Global Health*, Uppsala University, Box 580, SE-751 23, Uppsala, Sweden. Email: thomas.dorlo@farmaci.uu.se

DOI: 10.1093/infdis/jiae413

Africa. VL patients showed 0.55-fold (95%CI: 0.41-0.74) lower capacity for paromomycin saturable reabsorption in renal tubules, and required a 1.44-fold (1.23-1.71) adjustment when relating renal clearance to creatinine-based eGFR. Miltefosine bioavailability in VL patients was lowered by 69% (62-76) at treatment start. Comparing PKDL to VL patients on the same regimen, paromomycin plasma exposures were 0.74-0.87-fold, while miltefosine exposure until the end of treatment day was 1.4-fold. These pronounced PK differences between PKDL and VL patients in eastern Africa highlight the challenges of directly extrapolating dosing regimens from one leishmaniasis presentation to another.

Key words: Paromomycin; Miltefosine; Post-kala-azar dermal leishmaniasis (PKDL); Visceral leishmaniasis (VL); Pharmacokinetics.

1. INTRODUCTION

Visceral leishmaniasis (VL), also known as kala-azar, is the most severe form of the neglected tropical parasitic disease leishmaniasis, and is fatal if left untreated [1]. Post-kala-azar dermal leishmaniasis (PKDL) is a complication of VL that appears as skin lesions months or even years after successful treatment of a primary VL infection [2]. The infected skin of PKDL patients can serve as a reservoir for parasites [3,4]. As a result, PKDL is believed to play a pivotal role in the transmission of VL, making the treatment of PKDL patients a crucial element in efforts to eliminate VL.

In eastern Africa, where VL is caused by *Leishmania donovani*, the current standard of care is a 17-day combination therapy of sodium stibogluconate and paromomycin (SSG/PM) [5,6]. A recent Phase III study demonstrated that a 14-day combination treatment of paromomycin and miltefosine shows similar efficacy as SSG/PM, suggesting its potential to replace the toxic SSG-based regimen [7]. Notably, within 6 months of successful SSG/PM treatment, 21% of VL cases develop PKDL in Sudan and Ethiopia [7]. There is no consensus on the optimal treatment for PKDL. In Sudan, the current practice is treatment with SSG for over 60 days, which is associated with life-threatening toxicities and requires long hospitalization [8]. In a recent clinical study on PKDL in Sudan, a short course of liposomal amphotericin B or paromomycin was combined with prolonged oral miltefosine, requiring shorter hospitalization while maintaining high efficacy [9].

The dosing regimen and rationale for treatment of PKDL is typically extrapolated from those used for VL, with an extended treatment period due to the slow recovery of skin lesions [2]. However, VL and PKDL patients exhibit marked differences in disease presentation and physiological status. In VL, parasites manifest mainly in macrophages in spleen, liver and bone marrow, while in PKDL, the parasites reside locally in the skin lesions. As a result, VL patients are systemically severely ill and usually suffer from fever, weight loss and hematological depletions, whereas PKDL patients generally maintain better overall health except for their skin condition. These distinctions could potentially result in variations in the pharmacokinetics (PK) of antileishmanial drugs and the relationships between drug exposure and response.

The PK of paromomycin and miltefosine have been studied in VL patients, yet no PK data was previously available for PKDL patients. Paromomycin, a highly hydrophilic aminoglycoside, is rapidly absorbed following intramuscular (IM) injection and primarily excreted unchanged via glomerular filtration [10,11]. Renal function, expected to be better in PKDL compared to VL patients [12], may influence the clearance of paromomycin. Previous population PK studies in VL patients demonstrated changes in miltefosine bioavailability over a four-week treatment period, with a decrease of 69-74% in the first week, probably due to malabsorption related to the systemic infection and/or malnourishment [13,14]. Whether this effect is specific to VL patients or also applies to PKDL patients is unknown. Consequently, directly applying dosing regimens from VL to PKDL patients may lead to bias, with potential dose adjustments required for PKDL patients.

To optimize dosing in PKDL patients, understanding the PK differences between PKDL and VL patients is crucial. This study aimed to characterize the systemic PK of paromomycin and miltefosine in PKDL and VL patients from eastern Africa and to identify disease-specific factors affecting PK.

2. METHODS

Details regarding the sampling schedule and bioanalysis assays are documented in the supplementary file (Supplementary S1).

2.1 Clinical trials and patients

Pharmacokinetic data were collected from a PKDL (NCT03399955)[9] and a VL clinical study (NCT03129646)[7] in eastern Africa. In both studies, patients were screened for HIV infection and a positive HIV diagnosis was an exclusion criterion. In the PKDL study, patients were given paromomycin 20 mg/kg/day intramuscularly for 14 days and oral miltefosine (allometric dosing) for 42 days (PM/MF arm) or liposomal amphotericin B (AmBisome®) 5 mg/kg/day intravenously at day 1, 3, 5 and 7 and oral miltefosine (allometric dosing) for 28 days (LAmB/MF arm). In the VL study, patients were given paromomycin 20 mg/kg/day intramuscularly for 14 days combined with oral miltefosine (allometric dosing) for 14 days or 28 days (PM/MF 14D and PM/MF 28D arms). Miltefosine allometric dosing was calculated according to patient's weight, height and sex, and was applied to patients weighing < 30 kg [15]. For patients weighing ≥ 30 kg, the allometric dose corresponded to the conventional dose of 2.5 mg/kg/day, with a maximum 150 mg/day. Therefore, patients weighing ≥ 30 to 44 kg received 100 mg/day and patients ≥ 45 kg received 150 mg/day.

2.2 Paromomycin population pharmacokinetic analysis

Previous population PK studies in VL patients in India and eastern Africa demonstrated a decrease in paromomycin clearance over time [16,17]. This time-varying kinetics observed in paromomycin is most likely associated with megalin-mediated tubular reabsorption. Aminoglycosides are

primarily eliminated through glomerular filtration, with a fraction of the drug accumulating in the proximal tubule via the megalin receptors on the apical surface [18,19]. Following binding and uptake by megalin, aminoglycosides undergo endocytosis and transfer into lysosomes, where they accumulate and may reach a critical threshold for release [20]. This reabsorption process is saturable and is associated with the development of kidney injury [20].

The renal clearance of paromomycin comprises glomerular filtration of the free drug fraction, tubular reabsorption, and tubular secretion processes, given by equation 1.

(Equation 1)

$$CL_R = fu * GFR - CL_{reabsorption} + CL_{secretion}$$

Where CL_R is the total renal drug clearance, fu is the fraction of the drug unbound to plasma proteins, GFR is the glomerular filtration rate, $CL_{reabsorption}$ is drug reabsorption from the renal tubule, and $CL_{secretion}$ is the drug clearance by tubular secretion. Assuming free paromomycin is solely cleared through glomerular filtration, $CL_{secretion}$ could be omitted. Additionally, $CL_{reabsorption}$ was assumed to return to the central compartment without being excreted from the renal tubule.

Since the true GFR is unknown, renal drug clearance was informed by an estimate of GFR based on serum creatinine ($eGFR_{SCr}$) measured at baseline and on day 14. For individuals aged ≥ 18 years, the race-neutral CKD-EPI formula (2021) was utilized [21], and for those <18 years, the Bedside Schwartz formula was used [22]. However, the existing formulas for calculating $eGFR_{SCr}$ do not consider variability in creatinine production rates [23], which might play an important role in malnourished/severely ill populations like PKDL and VL patients. To evaluate this, $eGFR_{SCr}$ was further adjusted by factors specific to VL and PKDL, and was calculated to an absolute individual value by adapting the outcome of these formulas to the individual BSA, as denoted in equation 2.

(Equation 2)

$$eGFR_{adjusted} = eGFR_{SCr} * \frac{BSA}{1.73} * \theta^{PKDL} * \theta^{VL}$$

In which adjustment factors θ^{PKDL} and θ^{VL} were estimated to describe the fractional difference between $eGFR_{SCr}$ and $eGFR_{adjusted}$ in PKDL and VL patients, respectively. This $eGFR_{adjusted}$ was further related to CL_R using equation 3, which is a simplification of equation 1.

(Equation 3)

$$CL_R = (fu * eGFR_{adjusted}) * (1 - FR)$$

Here, fu was fixed to 0.67 based on protein-binding of paromomycin in literature [11] , and FR represents the fraction of drug reabsorbed from the renal tubules, accounting for the negative

contribution to clearance. $CL_{reabsorption}$ is derived from equation 4, in which the saturable reabsorption process, mediated by megalin receptors binding, was characterized using a maximal binding capacity (B_{max}) model represented by equation 5.

(Equation 4)

$$CL_{reabsorption} = \left(fu * eGFR_{adjusted}\right) * FR * \left(1 - \frac{A_{tubular}}{B_{max}}\right)$$

(Equation 5)

$$\frac{dA_{tubular}}{dt} = \left(\frac{CL_{reabsorption}}{V_C}\right) * A_{Central} * - k_{out} * A_{tubular}$$

In equation 4, B_{max} represents the maximal capacity for drug accumulation in the tubular compartment and $A_{tubular}$ is the drug amount in this compartment at given time point. In equation 5, the first-order rate constant of megalin-mediated reabsorption was obtained by dividing the $CL_{reabsorption}$ by the volume of distribution of the central compartment (V_C) and k_{out} describes the first-order rate constant for drug release from the tubular compartment to the central compartment. Factors that might affect the amount of megalin receptors and the drug-megalin interaction, including severity of the disease (VL relative to PKDL), body weight, age, sex, z-score, and albumin, were evaluated as covariates on B_{max}.

2.3 *Miltefosine* population pharmacokinetic analysis

The population PK of miltefosine in VL patients from eastern Africa has been relatively well studied, and we used previously developed models as a starting point [13–15]. Two covariates on relative oral bioavailability (F) found in previous models were evaluated sequentially. Firstly, it was tested whether disease specific differences were present in the previously observed reduced F during the first week of treatment. Secondly, the potential effect of cumulative miltefosine dose on F were examined [13–15]. Additionally, since miltefosine is prone to interact with lipids, the potential interaction of LAmB with miltefosine was evaluated in PKDL patients. Details regarding the miltefosine structural model and covariate analysis are documented in the supplementary file (Supplementary S2).

2.4 Exposure and target attainment

Secondary PK parameters for paromomycin and miltefosine were calculated using the individual estimates of the final PK models. Paromomycin exposure was determined by the area under the plasma concentration-time curve (AUC) from treatment start to day 1 ($AUC_{0\text{-}D1}$), day 14 ($AUC_{0\text{-}D14}$), and infinity ($AUC_{0\text{-}inf}$). Miltefosine exposure was expressed by the AUC from start until day 7 ($AUC_{0\text{-}D7}$), last dosing day ($AUC_{0\text{-}Dlast}$), and infinity ($AUC_{0\text{-}inf}$). The time point at which the miltefosine concentration reached the *in vitro* susceptibility value EC_{90} (TEC_{90}) and the total time period that miltefosine concentration was above the EC_{90} (Time > EC_{90}) were calculated. The EC_{90}

value of 10.6 mg/L was selected based on intracellular amastigote *in vitro* susceptibility testing of *Leishmania donovani* [14].

2.5 Analysis software and model evaluation

Population PK analysis was performed using the nonlinear mixed-effects modelling program NONMEM (version 7.5; ICON Development Solutions, Ellicott City, MD), aided by Perl-speaks-NONMEM (PsN, version 5.0) and Pirana (version 2.9.9) for run deployment [24,25]. Model parameters were estimated using the first-order conditional estimation with interaction (FOCE-I) method. Inter-individual variability (IIV) in PK parameters was estimated with an exponential variance model and residual unexplained variability was estimated with a proportional error model. Individual PK parameters were obtained by maximum a posterior Bayesian estimation using POSTHOC option of NONMEM.

Model adequacy was guided by physiological plausibility, statistical significance and graphical evaluation. The change in objective function value (OFV), which equals minus two times the log-likelihood, was used to define statistical significance between hierarchical models following a Chi-square distribution with 1 degree of freedom. A decrease in OFV of ≥ 3.84, representing a p-value of < 0.05, was considered statistically significant. Goodness-of-fit plots were used to assist graphical evaluation using R (version 4.0) and Xpose (version 4). A visual predictive check (VPC) and sampling importance resampling (SIR) were performed to assess the predictive performance and the parameter precision with 95% confidence intervals (CI) for the final model [26,27].

3. RESULTS

3.1 Patients and data

Demographic characteristics of the included patients are presented in Table 1. Plasma concentration-time profiles of paromomycin and miltefosine are depicted in Supplementary Figures S1 and S2, respectively. A total of 328 paromomycin observations and 1516 miltefosine observations were collected in 109 PKDL and 264 VL patients (Table 1A). The majority of the patients were children and adolescents aged ≤18 years, accounting for 96% and 72% of included PKDL and VL patients, respectively. Severely malnourished patients were excluded from both clinical trials. For both VL and PKDL, the pediatric populations were mildly malnourished, as reflected by z-scores with interquartile range between -2.0 and -0.5 (Table 1B). As both populations were from extremely poor area and were to a large extent malnourished, BMI was not considered as an indicator for disease status. The distribution of body weight and BMI were similar between PKDL and VL patients for the different age groups, indicating comparable body size (Table 1B). The median albumin level and neutrophil count at baseline were 0.71- and 0.34-fold lower, respectively, in VL versus PKDL patients, while the creatinine level was 2-fold higher (Table 1C), confirming expected disease-specific differences in these hematological and biochemical variables.

3.2 Pharmacokinetics of paromomycin in PKDL and VL

Plasma concentration-time profiles of paromomycin were best described by a three-compartment model with a saturable compartment, characterizing renal clearance processes, as depicted in Figure 1. The overall clearance from the central compartment was subsequently divided into two fractions: CL_R representing total renal clearance (Equation 3) and $CL_{reabsorption}$ representing saturable tubular reabsorption (Equation 4). The parameter estimates of the final model are summarized in Table 2.

Variabilities in CL_R between individuals and throughout the 14-day treatment period were adequately described by $eGFR_{adjusted}$, where the disease-specific adjustment θ^{PKDL} was estimated and subsequently fixed to 1, while θ^{VL} was 1.44 (95%CI: 1.23-1.71), accounting for differences in creatinine production. This result suggested that approximating CL_R of paromomycin using solely serum creatinine-based eGFR is feasible in PKDL patients, while this may lead to underestimation of CL_R in VL patients by 44%.

Incorporating a saturable compartment to reflect paromomycin reabsorption via megalin significantly improved the model fit and explained the time-dependent trends (details in Supplementary S3). In the final model, FR was estimated at 0.3 (95%CI:0.2-0.39), the maximal first-order rate constant for megalin-mediated drug reabsorption was 0.13 1/h, and k_{out} for drug release into central compartment was estimated at 0.009 1/h (95%CI: 0.005-0.015). Severity of the disease was a significant covariate on B_{max}, indicating that the maximum capacity for paromomycin accumulation in the tubular compartment was 0.55-fold (95%CI: 0.41-0.74) lower in VL patients compared to PKDL patients. No additional significant covariates were found to explain variability in B_{max}.

3.3 Pharmacokinetics of miltefosine in PKDL and VL

In line with previous studies, miltefosine concentration-time profiles were best described by a two-compartment model with first-order absorption and first-order elimination. The parameter estimates of the final model are summarized in Table 3. Nonlinearities in miltefosine PK were identified and were best described by three effects on F: disease-related reduction in the first week ($COV_{F,W1}$), cumulative dose ($COV_{F,CD}$), and a drug-drug interaction with LAmB ($COV_{F,LAmB}$). Details are further elaborated in supplementary file (Supplementary S4).

In the concentration-time profiles, a large difference in drug accumulation and exposure between VL patients and PKDL patients was observed in the first week of treatment (Supplementary Figure S2). In VL patients, F in the first week of treatment decreased by 69% (95% CI: 62-76). However, in PKDL patients, a decrease in F was not identified in the first week of treatment; therefore, $COV_{F,W1}$ was fixed to 0. In addition to the difference in F, the rate of absorption (k_a) in PKDL and VL was 5.43 day^{-1} (95% CI: 4.54-6.26) and 0.99 day^{-1} (95%CI: 0.84-1.17), respectively, indicating a

much longer absorption half-life in VL patients. Simulated concentration-time profiles for a typical PKDL patient and a VL patient receiving a 28-day miltefosine regimen are presented in Figure 2. Since PKDL patients are not affected by a systemic parasitic infection, the relatively low k_a and F at treatment start found only in VL patients are consistent with previous hypotheses about systemic VL infection-related malabsorption [28,29]. Despite a similar daily dosing regimen, in the first week median miltefosine concentration was 12% lower in PKDL patients who received LAmB-MF than in patients receiving PM-MF (Supplementary Figure S2). LAmB was found to reduce miltefosine's F by 8.6% (95% CI: 2-15) in the first week.

3.4 Exposure and target attainment in PKDL and VL

Plasma exposures and target attainment of paromomycin and miltefosine are summarized in Table 4 and Table 5, respectively. In the populations studied, median paromomycin $AUC_{0\text{-}D1}$ and $AUC_{0\text{-}D14}$ in PKDL patients was 0.74- and 0.86-fold lower than in VL patients, respectively. Miltefosine $AUC_{0\text{-}D7}$ irrespective to treatment arms was 3.7-fold higher in PKDL patients compared to VL patients (median 98.6 mg*day/L in PKDL and 26.1 mg*day/L in VL). In the 28-day miltefosine treatment arms, $AUC_{0\text{-}D28}$ was 1.4-fold higher in PKDL patients compared to VL patients. Due to differences in initial drug accumulation, TEC_{90} was 2 and 9 days after the treatment start in PKDL and VL patients, respectively.

4. DISCUSSION

Large and clinically relevant differences in drug exposure and PK parameters for paromomycin and miltefosine between PKDL and VL patients in eastern Africa were identified and quantified for the first time. In PKDL patients, the $AUC_{0\text{-}D1}$ of paromomycin was 0.74-fold lower, while $AUC_{0\text{-}D28}$ of miltefosine was 1.4-fold higher compared to VL patients. These considerable differences in exposure indicate that dosing regimens cannot be directly extrapolated from VL to PKDL, especially in eastern Africa.

The reduced plasma exposure to paromomycin in PKDL patients is associated with greater drug accumulation in the renal tubule and higher renal clearance, attributed to better renal function at baseline. This lower systemic exposure could potentially account for the lower occurrence of ototoxicity in PKDL patients. For instance, ear and labyrinth disorders were observed in 5.3% of VL patients but were absent in PKDL patients in the clinical trials [7,9]. While the current paromomycin-based regimen was shown to be effective in managing PKDL patients from eastern Africa, this suggests that higher paromomycin dosages might be tolerable in PKDL patients compared to VL patients [9]. On the other hand, the higher F for miltefosine found in PKDL patients is likely due to better gastrointestinal absorption, which resulted in increased miltefosine

exposure and faster achievement of EC_{90}. This, in turns, implies the possibility of a shorter miltefosine treatment duration in PKDL patients from eastern Africa.

In the paromomycin model, the time-dependent exposure observed was explained by alterations in renal function, partly influenced by saturable tubular reabsorption. After glomerular filtration, aminoglycosides are reabsorbed through megalin receptors on the apical tubular surface and accumulate in cell lysosomes, which can result in further nephrotoxicity [18–20]. In VL patients, B_{max} was 0.55-fold (95%CI: 0.41-0.73) lower than in PKDL patients, explaining the slower decrease in paromomycin concentration observed within 4 hours post-dose. Renal involvement, commonly observed in VL [12], could contribute to this lower reabsorption capacity found in VL patients, as symptoms like albuminuria can signify tubular stress and decreased activity of megalin, leading to decreased tubular reabsorption [30]. Although it remains unclear whether aminoglycosides renal toxicity is related to local drug concentration or drug release from lysosomes [18–20], the lower reabsorption capacity in VL patients might suggest a reduced tolerance for aminoglycoside-induced renal toxicity. The framework of the current model can be extended to other aminoglycosides to further explore the relationship between drug accumulation in renal tubules and drug-induced toxicity.

A decrease in the renal clearance of paromomycin was observed during the 14-day treatment period in both PKDL and VL patients. In PKDL patients, the renal clearance aligned with creatinine-based eGFR, whereas in VL patients, correlating renal clearance with creatinine-based eGFR required a disease-specific correction of 1.44-fold. This discrepancy suggests that the measured serum creatinine level did not accurately reflect the renal function, particularly in this severely ill and malnourished population. This could be attributed to a lack of validated equations for estimating GFR based on serum creatinine in this particular population, wherein the deviating production of creatinine is not accurately accounted for [23]. The validity of current creatinine-based eGFR estimation methods in similar populations has been questioned previously [31].

For miltefosine, F was decreased by 69% (95%CI: 62-76) in VL patients in the first week of treatment, while in PKDL patients no initial decrease in F was noticeable. The k_a in VL patients was 0.99 day^{-1} (95CI: 0.84-1.17), comparable to previously reported values of 0.4 -1.6 day^{-1} [13–15]. The k_a in PKDL patients was described for the first time, equal to 5.43 day^{-1} (95%CI: 4.54-6.26), which was much faster than the VL patients, but comparable to the k_a of 8.64 day^{-1} reported for cutaneous leishmaniasis patients [32]. The reduced F and slower k_a imply poor gastrointestinal absorption in VL patients, probably owing to a more severe disease status or, potentially, a local gastrointestinal effect of the systemic *Leishmania* infection [33].

Co-administration of LAmB was found to lower miltefosine exposure by around 10%, suggesting a potential drug-drug interaction between miltefosine and LAmB. The decreased miltefosine exposure could potentially be associated with the higher frequency of vomiting observed in the LAmB/MF arm of PKDL trial, which mainly occurred during the first two weeks of treatment, even though the drug was re-administered in case of vomiting [9]. Beside this, free or micellular

miltefosine can theoretically be incorporated into the liposomes of LAmB [34,35]. However, this additional miltefosine clearance route might actually be beneficial for increased miltefosine target-site delivery and activity as liposomes are preferentially phagocytized by parasite-infected macrophages [36].

This study illustrates and highlights the difficulty of directly extrapolating dosing regimens between VL and the various other dermal clinical presentations of leishmaniasis, particularly for orally administered and renally cleared drugs. Moreover, various disease-specific mechanisms affecting the absorption, distribution and elimination of paromomycin and miltefosine were identified and characterized. These findings should be taken into consideration when developing new treatments for leishmaniasis, emphasizing the importance of characterizing PK and PK/PD relationships across different clinical manifestations of the disease. To optimize dosing of paromomycin and miltefosine for PKDL patients, it is essential to further establish exposure-response relationships, with a focus on the relevance of drug exposure within skin target site.

Funding

This work was supported by the European and Developing Countries Clinical Trials Partnership Association (EDCTP2) programme supported by the European Union (grant number RIA2016S-1635 AfriKADIA); the Dutch Ministry of Foreign Affairs (Directeur-generaal Internationale Samenwerking, DGIS), the Netherlands; the Federal Ministry of Education and Research (Bundesministerium für Bildungund Forschung, BMBF) through KfW, Germany; Medicor Foundation; Médecins sans Frontières International; Swiss Agency for Development and Cooperation (SDC), Switzerland; UK aid, UK; and other private individuals and foundations. T.D. was supported by the Dutch Research Council (NWO/ZonMw; project 91617140) and the Swedish Research Council (VR 2022-01251).

Conflict of Interest: None to declare.

Acknowledgment: The authors thank the patients involved in this study and their families and communities for their willingness to participate in the trial; all co-investigators, nurses, laboratory personnel, and hospital administrators who allowed the authors to conduct the study in their respective study sites; and staff at the five Leishmaniasis East Africa Platform (LEAP) sites and two Doctors Without Borders (Médecins Sans Frontières, MSF) sites: Kacheliba in Kenya; Amudat in Uganda; Doka, Umelkher, and Tabarakallah (MSF) in Sudan; and Gondar and Abdurafi (MSF) in Ethiopia. DNDi also thanks UK aid, Médecins sans Frontières International, and the Swiss Agency for Development and Cooperation (SDC) for supporting its overall mission

References

1. Harhay MO, Olliaro PL, Vaillant M, et al. Who is a typical patient with visceral leishmaniasis? Characterizing the demographic and nutritional profile of patients in Brazil, East Africa, and South Asia. Am J Trop Med Hyg. Am J Trop Med Hyg; **2011**; 84(4):543–550.

2. Zijlstra EE, Musa AM, Khalil EAG, Hassan IM El, El-Hassan AM. Post-kala-azar dermal leishmaniasis. Lancet Infect. Dis. Lancet Infect Dis; 2003. p. 87–98.
3. Mondal D, Bern C, Ghosh D, et al. Quantifying the Infectiousness of Post-Kala-Azar Dermal Leishmaniasis Toward Sand Flies. Clin Infect Dis an Off Publ Infect Dis Soc Am. United States; **2019**; 69(2):251–258.
4. Singh OP, Tiwary P, Kushwaha AK, et al. Xenodiagnosis to evaluate the infectiousness of humans to sandflies in an area endemic for visceral leishmaniasis in Bihar, India: a transmission-dynamics study. The Lancet Microbe. England; **2021**; 2(1):e23–e31.
5. Wasunna M, Musa A, Hailu A, et al. The Leishmaniasis East Africa Platform (LEAP): strengthening clinical trial capacity in resource-limited countries to deliver new treatments for visceral leishmaniasis. Trans R Soc Trop Med Hyg. Oxford University Press; **2016**; 110(6):321.
6. Kimutai R, Musa AM, Njoroge S, et al. Safety and Effectiveness of Sodium Stibogluconate and Paromomycin Combination for the Treatment of Visceral Leishmaniasis in Eastern Africa: Results from a Pharmacovigilance Programme. Clin Drug Investig. Springer; **2017**; 37(3):259–272.
7. Musa AM, Mbui J, Mohammed R, et al. Paromomycin and Miltefosine Combination as an Alternative to Treat Patients with Visceral Leishmaniasis in Eastern Africa: A Randomized, Controlled, Multicountry Trial. Clin Infect Dis. Clin Infect Dis; **2023**; 76(3):E1177–E1185.
8. Musa AM, Khalil EAG, Younis BM, et al. Treatment-based strategy for the management of post-kala-azar dermal leishmaniasis patients in the Sudan. J. Trop. Med. Egypt; 2013. p. 708391.
9. Younis BM, Mudawi Musa A, Monnerat S, et al. Safety and efficacy of paromomycin/miltefosine/liposomal amphotericin B combinations for the treatment of post-kala-azar dermal leishmaniasis in Sudan: A phase II, open label, randomized, parallel arm study. PLoS Negl Trop Dis. United States; **2023**; 17(11):e0011780.
10. Institute for One World Health. Application for inclusion of paromomycin in the WHO Model List of Essential Medicines. 2006.
11. Talbert RL. Drug dosing in renal insufficiency. J. Clin. Pharmacol. John Wiley & Sons, Ltd; 1994. p. 99–110.
12. Clementi A, Battaglia G, Floris M, Castellino P, Ronco C, Cruz DN. Renal involvement in leishmaniasis: a review of the literature. NDT Plus. England; **2011**; 4(3):147–152.
13. Palic S, Kip AE, Beijnen JH, et al. Characterizing the non-linear pharmacokinetics of miltefosine in paediatric visceral leishmaniasis patients from Eastern Africa. J Antimicrob Chemother. J Antimicrob Chemother; **2020**; 75(11):3260–3268.
14. Dorlo TPC, Kip AE, Younis BM, et al. Visceral leishmaniasis relapse hazard is linked to reduced miltefosine exposure in patients from Eastern Africa: A population pharmacokinetic/pharmacodynamic study. J Antimicrob Chemother. Oxford University Press; **2017**; 72(11):3131–3140.
15. Dorlo TPC, Huitema ADR, Beijnen JH, Vries PJ De. Optimal dosing of miltefosine in children and adults with visceral leishmaniasis. Antimicrob Agents Chemother. American Society for Microbiology; **2012**; 56(7):3864–3872.
16. Verrest L, Roseboom IC, Wasunna M, et al. Population pharmacokinetics of a combination of miltefosine and paromomycin in Eastern African children and adults with visceral leishmaniasis. Thesis Luka Verrest.
17. Verrest L, Wasunna M, Kokwaro G, et al. Geographical Variability in Paromomycin Pharmacokinetics Does Not Explain Efficacy Differences between Eastern African and Indian

Visceral Leishmaniasis Patients. Clin Pharmacokinet. Clin Pharmacokinet; **2021**; 60(11):1463–1473.
18. Mingeot-Leclercq MP, Tulkens PM. Aminoglycosides: Nephrotoxicity. Antimicrob. Agents Chemother. American Society for Microbiology (ASM); 1999. p. 1003–1012.
19. Lopez-Novoa JM, Quiros Y, Vicente L, Morales AI, Lopez-Hernandez FJ. New insights into the mechanism of aminoglycoside nephrotoxicity: An integrative point of view. Kidney Int. Elsevier; 2011. p. 33–45.
20. Perazella MA. Pharmacology behind Common Drug Nephrotoxicities. Clin J Am Soc Nephrol. American Society of Nephrology; **2018**; 13(12):1897.
21. Inker LA, Eneanya ND, Coresh J, et al. New Creatinine- and Cystatin C-Based Equations to Estimate GFR without Race. N Engl J Med. United States; **2021**; 385(19):1737–1749.
22. Schwartz GJ, Muñoz A, Schneider MF, et al. New equations to estimate GFR in children with CKD. J Am Soc Nephrol. J Am Soc Nephrol; **2009**; 20(3):629–637.
23. Waikar SS, Sabbisetti VS, Bonventre J V. Normalization of urinary biomarkers to creatinine during changes in glomerular filtration rate. Kidney Int. Kidney Int; **2010**; 78(5):486–494.
24. Lindbom L, Ribbing J, Jonsson EN. Perl-speaks-NONMEM (PsN)--a Perl module for NONMEM related programming. Comput Methods Programs Biomed. Comput Methods Programs Biomed; **2004**; 75(2):85–94.
25. Keizer RJ, Benten M van, Beijnen JH, Schellens JHM, Huitema ADR. Piraña and PCluster: A modeling environment and cluster infrastructure for NONMEM. Comput Methods Programs Biomed. **2011**; 101(1):72–79.
26. Bergstrand M, Hooker AC, Wallin JE, Karlsson MO. Prediction-Corrected Visual Predictive Checks for Diagnosing Nonlinear Mixed-Effects Models. AAPS J. Springer; **2011**; 13(2):143.
27. Dosne AG, Bergstrand M, Karlsson MO. An automated sampling importance resampling procedure for estimating parameter uncertainty. J Pharmacokinet Pharmacodyn. Springer New York LLC; **2017**; 44(6):509–520.
28. Viteri FE, Flores JM, Alvarado J, Béhar M. Intestinal malabsorption in malnourished children before and during recovery. Relation between severity of protein deficiency and the malabsorption process. Am J Dig Dis. Am J Dig Dis; **1973**; 18(3):201–211.
29. Krishnaswamy K. Drug Metabolism and Pharmacokinetics in Malnourished Children. Clin Pharmacokinet. Clin Pharmacokinet; **1989**; 17(1):68–88.
30. Thompson LE, Joy MS. Endogenous markers of kidney function and renal drug clearance processes of filtration, secretion, and reabsorption. Curr Opin Toxicol. Netherlands; **2022**; 31.
31. Fabian J, Kalyesubula R, Mkandawire J, et al. Measurement of kidney function in Malawi, South Africa, and Uganda: a multicentre cohort study. Lancet Glob Heal. Lancet Glob Health; **2022**; 10(8):e1159–e1169.
32. Dorlo TPC, Thiel PPAM Van, Huitema ADR, et al. Pharmacokinetics of miltefosine in old world cutaneous leishmaniasis patients. Antimicrob Agents Chemother. American Society for Microbiology; **2008**; 52(8):2855–2860.
33. Hatton GB, Madla CM, Rabbie SC, Basit AW. Gut reaction: impact of systemic diseases on gastrointestinal physiology and drug absorption. Drug Discov Today. England; **2019**; 24(2):417–427.
34. Seifert F. Local steps in an international career: A Danish-style consensus conference in Austria. Public Underst. Sci. Antimicrob Agents Chemother; 2006. p. 73–88.

35. Barratt G, Saint-Pierre-Chazalet M, Loiseau P. Cellular transport and lipid interactions of miltefosine. Curr Drug Metab. Curr Drug Metab; **2009**; 10(3):247–255.
36. Kelly C, Jefferies C, Cryan S-A. Targeted Liposomal Drug Delivery to Monocytes and Macrophages. J Drug Deliv. J Drug Deliv; **2011**; 2011:1–11.

TABLES

Table 1. Patient demographics

A Treatment details

Population	**PKDL**	**VL**
Total no. of patients	109	264
Included no. in PK analysis		
PM model	14	26
MF model	109	264
PKDL Treatment regimens, n (%)		
LAMB + MF 28 days	54 (49.5%)	
PM + MF 42 days	55 (50.5%)	
VL Treatment regimens, n (%)		
PM + MF 28 days		167 (63.3%)
PM + MF 14 days		97 (36.7%)

B Baseline characteristics (median [interquartile range, IQR])

Population	**PKDL**			**VL**		
Age range (n)	**Age ≤ 10 (N=83)**	**10 < Age ≤ 18 (N=22)**	**Age >18 (N=4)**	**Age ≤ 10 (N=130)**	**10 < Age ≤ 18 (N=61)**	**Age >18 (N=73)**
Age (years)	8.00 [6.00, 9.00]	12.0 [11.0, 13.8]	25.5 [22.8, 27.8]	8.00 [6.00, 9.75]	13.0 [11.0, 15.0]	23.0 [21.0, 28.0]
Body weight (kg)	21.0 [18.0, 24.8]	35.0 [31.0, 40.8]	63.5 [55.5, 71.0]	20.5 [17.1, 25.0]	35.0 [32.0, 41.0]	51.0 [47.0, 54.0]
Height (cm)	121 [113, 129]	148 [142, 157]	178 [174, 183]	123 [113, 132]	149 [140, 158]	170 [165, 176]
Body mass index (kg/m^2)	14.3 [13.6, 15.0]	15.8 [15.2, 16.8]	20.0 [18.4, 21.2]	13.5 [13.1, 14.4]	15.6 [14.9, 17.0]	17.8 [16.5, 18.7]
Body surface area (m^2)	0.87 [0.74, 0.95]	1.22 [1.12, 1.37]	1.79 [1.67, 1.92]	0.86 [0.74, 0.98]	1.21 [1.10, 1.35]	1.58 [1.51, 1.66]

Fat-free-mass (kg)	17.4 [14.7, 20.1]	28.3 [24.7, 35.2]	53.4 [48.3, 58.5]	17.1 [14.3, 20.7]	29.0 [25.9, 35.5]	44.9 [42.5, 48.0]
Z-score [a]	-1.19 [b] [-1.84, -0.58]	-1.18 [c] [-1.55, -0.56]	-	-1.04 [b] [-1.78, -0.52]	-1.63 [c] [-2.04, -1.02]	-
Male (n, %)	47 (56.6%)	18 (81.8%)	4 (100%)	89 (68.5%)	52 (85.2%)	72 (98.6%)

[a] The z-scores were calculated using the WHO Child Growth Standards for children aged between zero and 60 months or the WHO Growth References for school-aged children and adolescents using R package "zscorer".
[b] For children aged below 10-years, z-scores were calculated based on weight-for-age.
[c] For children aged between 10 and 18 years, z-scores were calculated based on body mass index-for-age.

C Laboratory examinations (median [interquartile range, IQR])

Population	PKDL (n=109)	VL (n=264)	p-value
Albumin (g/L)	38.8 [36.5, 41.4]	27.4 [23.3, 32.4]	<0.001
Creatinine (mg/dL)			
Baseline	0.4 [0.2, 0.5]	0.8 [0.6, 1.0]	<0.001
Day 14	0.6 [0.5, 0.8]	0.8 [0.6, 1.1] [b]	<0.001
Absolute eGFR (ml/min)[a]			
Baseline	78.5 [55.2, 108]	56.6 [33.1, 98.3]	<0.001
Day 14	50.3 [34.2, 65.9]	50.2 [30.8, 90.2] [b]	0.597
Absolute Neutrophil (x10^3/µL)			
Baseline	2.91 [2.45, 3.56]	1.00 [0.700, 1.40]	<0.001
Day 14	3.42 [2.70, 4.32]	2.20 [1.70, 2.80]	<0.001

[a] Estimated glomerular filtration rate (eGFR) is calculated from race-neutral CKD-EPI formula (2021) for age ≥ 18 years and Bedside Schwartz formula for age < 18 years.
[b] Data was available in n=262 patients.
[c] The Mann-Whitney U test was used to evaluate if there is a statistically significant difference between the medians of two groups. A p-value ≤ 0.05 indicates a significant difference in the median between the groups.

Table 2. Paromomycin final model parameter estimates

Paromomycin fraction unbound	Unit	Estimate	95%CI
Rate of absorption (k_a)	1/h	2.5	2.05-3.33
Fraction tubular reabsorption (FR)	-	0.3	0.2-0.39
Total renal clearance (CL_R) [a]	L/h	2.3	-
Reabsorption from renal tubules ($CL_{reabsorption}$) [a]	L/h	0.98	
Volume of central compartment [b] (Vc/F)	L	6.92	6.55-7.3

Inter-compartmental clearance [b] (Q/F)	L/h	0.12	0.10-0.15
Volume of peripheral compartment [b] (Vp/F)	L	20.2	7.6-38.7
Rate constant for drug release from renal tubules (k_{out})	1/h	0.009	0.005-0.015
Maximal drug accumulation in tubules (B_{max})	mg	85	50-134
Fold difference in B_{max} (VL relative to PKDL)		0.55	0.41-0.74
Factor adjusting creatinine-based eGFR to renal clearance [c]	-		
In PKDL		1 (fixed)	
In VL	-	1.44	1.23-1.71
Between subject variability (BSV) in Vc/F	CV%	11	6-15
Between occasion variability (BOV) in adjusted eGFR	CV%	40	35-49
Residual proportional error	CV%	17	15-19

[a] CL_R and $CL_{reabsorption}$ were calculated by $fu*eGFR_{adjusted}*(1-FR)$ and $fu*eGFR_{adjusted}*FR$, respectively, using individual Empirical Bayes estimates of the final model. The values are presented as median.
[b] Allometric scaled based weight with power exponent of 0.75 for clearance and 1 for volume of distribution. Estimate is given for a standardized body weight of 25 kg.
[c] Creatinine-based eGFR is calculated from the race-neutral CKD-EPI formula (2021) for aged ≥ 18 years [21], and the Bedside Schwartz formula for age <18 years [22].

Table 3. Miltefosine final model parameter estimates

	Unit	Estimate	95%CI
Absorption rate in PKDL (k_a PKDL)	1/day	5.43	4.54-6.26
Absorption rate in VL (k_a VL)	1/day	0.99	0.84-1.17
Clearance [a] (CL/F)	L/day	1.53	1.4-1.66
Volume of central compartment [a] (V2/F)	L	13.8	12.66-14.89
Inter-compartmental clearance (Q/F)	L/day	0.039	0.032-0.049
Volume of peripheral compartment [a] (V3/F)	L	2.01	1.69-2.54
F after a week of treatment	%	100 (Fixed)	
Relative decrease in F during the first week of treatment ($COV_{F,W1}$)			
PKDL patients	%	0 (Fixed)	
VL patients	%	69	62-76
Co-administration of LAmB ($COV_{F,LAmB}$)	%	8.6	2-15
Exponent of power relationship between cumulative MF dose and F ($COV_{F,CD}$)	-	-0.13	(-0.16) - (-0.11)
Between subject variability (IIV)			
CL/F	CV%	20	17-22
V2/F	CV%	13[b]	-
$COV_{F,W1}$ in VL patients	CV%	71	61-83
Residual proportional error	CV%	31	30-33

[a] Allometric scaled based on fat-free mass with power exponent of 0.75 for clearance and 1 for volume of distribution. Estimate is given for a standardized fat free mass of 25 kg

[b] IIV in V2/ F was not unidentifiable, but high correlation between CL/F and V2/F was suggested by SIR result. Therefore, the same ETA distribution was assumed for CL/F and V/F, and a scaling factor of 0.45 was estimated.

Table 4. Paromomycin plasma exposure and target attainment (median [interquartile range, IQR])

	PKDL (n=14)	VL (n=26)
$AUC_{0\text{-}D1}$ (mg*hr/L)	127 [117, 148]	171 [124, 207]
$AUC_{0\text{-}D14}$ (mg*hr/L)	2370 [2130, 2420]	2770 [2380, 3440]
$AUC_{0\text{-}inf}$ (mg*hr/L)	2460 [2220, 2500]	2840 [2430, 3520]

AUC: Area under the plasma concentration-time curve.
Both PKDL and VL patients received 14 days of 20 mg/kg paromomycin.

Table 5. Miltefosine exposure and target attainment (median [interquartile range, IQR])

	PKDL		VL	
Treatment regimen	LAMB + 28-day MF (n=54)	PM + 42-day MF (n=55)	PM + 14-day MF (n=167)	PM + 28-day MF (n=97)
$AUC_{0\text{-}D7}$ (mg*day/L)	95.6 [89.9, 103]	107 [74.4, 159]	28.2 [21.3, 34.9]	24.9 [22.1, 27.6]
$AUC_{0\text{-}Dlast}$ (mg*day/L)	720 [658, 762]	1130 [1010, 1260]	129 [113, 154]	514 [452, 548]
$AUC_{0\text{-}inf}$ (mg*day/L)	991 [885, 1090]	1410 [1260, 1570]	352 [301, 415]	808 [693, 906]
TEC_{90} (days)	2.10 [2.01, 2.30]	2.06 [1.95, 2.17]	8.69 [7.82, 9.33]	9.11 [8.78, 9.59]
Time > EC_{90} (days)	34.4 [33.2, 35.7]	48.1 [46.5, 50.1]	12.7 [10.9, 14.9]	28.7 [26.6, 31.2]

AUC: Area under the plasma concentration-time curve.
$AUC_{0\text{-}Dlast}$: Area under the plasma concentration-time curve from start until the end of last dosing day.
EC_{90}: 90% effective miltefosine concentration, equivalent to 10.6 µg/mL.
TEC_{90}: Time point that the miltefosine plasma concentration reached the *in vitro* susceptibility value EC_{90}.
Time > EC_{90}: Total time period that the miltefosine concentration was above the *in vitro* susceptibility value EC_{90} from the treatment start until time infinity.

FIGURES

Figure 1. Structure of the final paromomycin model. The overall clearance from the central compartment was divided into two components: total renal clearance (CL_R) and tubular reabsorption ($CL_{reabsorption}$), where the fraction of reabsorption is denoted as FR. $eGFR_{adjusted}$ represent creatinine-based estimates of GFR adjusted for disease-specific creatine production. k_a, rate of absorption; Vc/F, volume of the central compartment; Q/F, inter-compartmental clearance; V3/F, volume of the peripheral compartment; k_{out}, first-order rate constant for drug release from tubule to central compartment; B_{max}, maximal drug accumulation in the saturable tubular compartment.

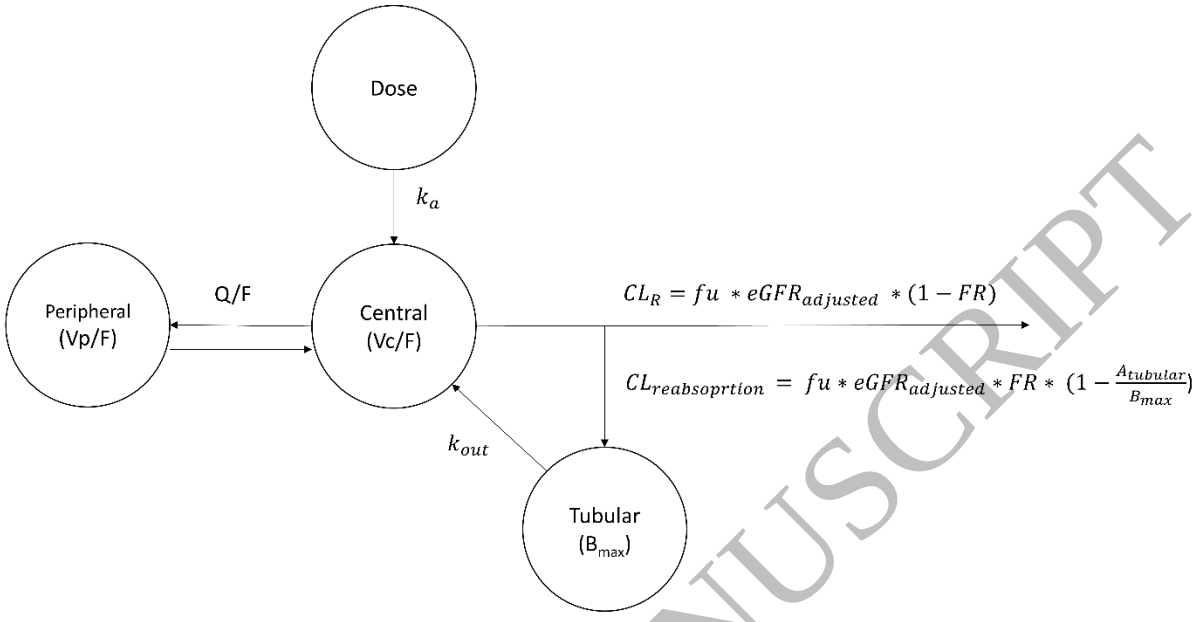

Figure 2. Simulated concentration-time profiles for a typical PKDL patient (red lines) and a VL patient (blue lines) with a fat-free mass of 25 kg receiving a 28-day miltefosine regimen. The black dashed line represents end of miltefosine treatment (Day 28). Miltefosine concentrations during the first week of treatment were lower in VL patients but approached levels similar to those in PKDL patients after the third week of treatment.